

High spatial resolution X-ray imaging detector at SACLA



Takashi Kameshima, Takaki Hatsui
SACLA
E-mail: kameshima@spring8.or.jp

Abstract

This poster presents a high resolution X-ray imaging detector developed and deployed at SACLA. The upgrade plans are also introduced for the enhancement of the field of view and the resolution. In resolution ranges of a few micrometer or less, an indirect X-ray imaging detector is generally used. This detection system consists of a scintillator, imaging optics, and an image sensor. In this imaging system, the spatial resolution is limited to be around 1 μm by the optical problems such as defocus light arising from outside of the depth of field and optical diffusion in the scintillator. To solve this, we have developed a novel-thin-film scintillator. A 5 μm -thick LuAG:Ce is directly formed on the 1-mm-thick non-doped LuAG. The fabricated scintillators have no adhesive layer and no pores causing the optical diffusion. We produced an indirect X-ray imaging detector equipped with the fabricated scintillator for evaluation of the resolving power. X-ray transmission images of 200 nm line-and-space patterns were successfully resolved. Also, the detector performance was demonstrated by visualizing the aluminum wiring lines with 300 nm width patterned in the inner layer of very large scaled integrated circuits (VLSI) [1]. Two types of the camera heads are deployed and designed to be capable of selecting optical configuration. The field of view is planned to be enlarged by implementing a large-format image sensor. We propose a solid immersion lens for resolution enhancement.

Introduction

Structure of lens-coupled indirect imaging detector

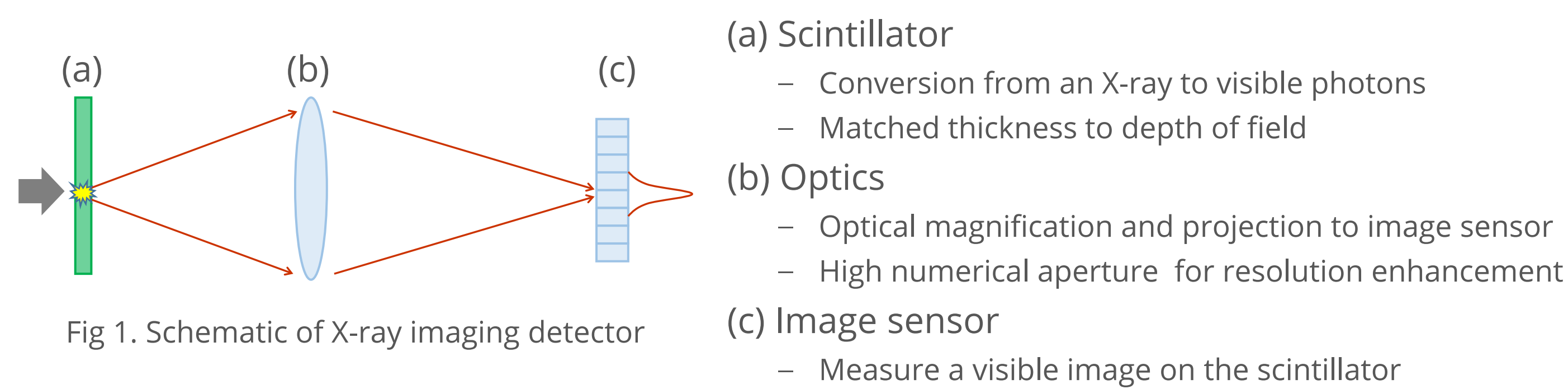


Fig. 1. Schematic of X-ray imaging detector

Resolution deterioration arising from optical diffusion

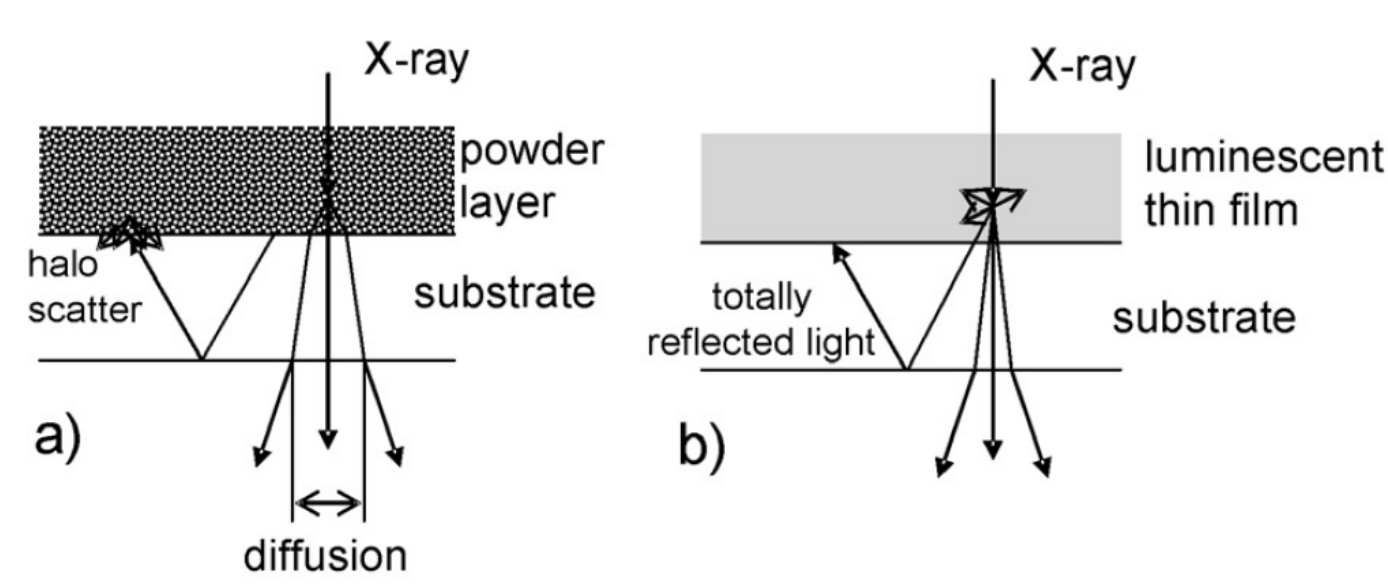


Fig. 2. Optical diffusion in the substrate

Optical diffusion caused by

- Pores
- Unmatched interface
- Distortion
- Rough surfaces
- X-ray damage of an adhesive layer
- X-ray damage of imaging optics

H. Graafsma and T. Martin, in *Advanced tomographic methods in materials research and engineering* 277 (2008)

To achieve diffraction-limited resolution, the detector should eliminate optical problems such as defocus light arising outside of depth of field, optical diffusion caused by opacity of light propagation path. Several thin-film fabrication methods are proposed to fulfill this and enhance resolution [2-7]. However, the deep sub-micron resolution performance was not reported.

Development & performance

Transparent ceramics technology

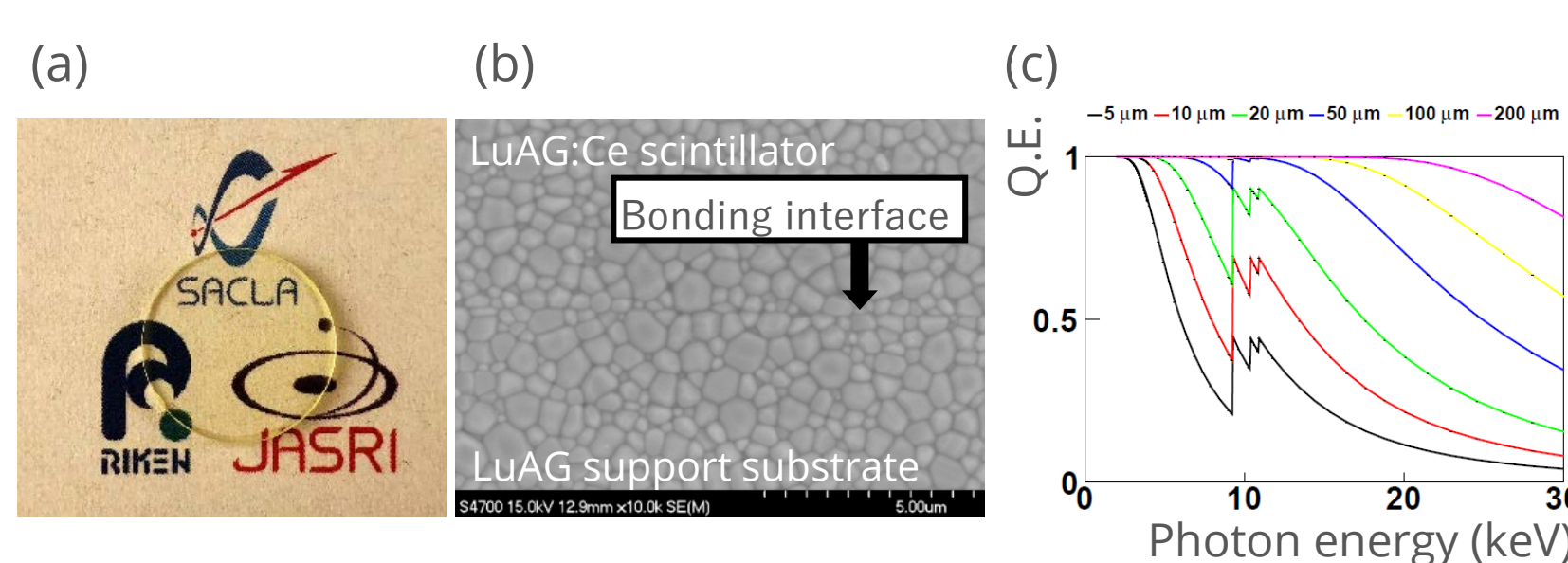


Fig. 3 (a) 5 μm -thick LuAG:Ce scintillator formed on the 1mm-thick non-doped LuAG
(b) SEM image of LuAG:Ce/LuAG composite at region of the bonding interface
(c) Quantum efficiency of LuAG

Fully densified LuAG grains, sub-nm grain boundary, and direct bonding provide scintillator property such as

- No pores
- Quasi-homogeneous refractive index
- Low distortion
- High radiation hardness
- High radiation shielding

This features exhibit near-laser-grade optical quality and permit high NA installation in tandem placement of the scintillator and objective [1].

Achieved performance

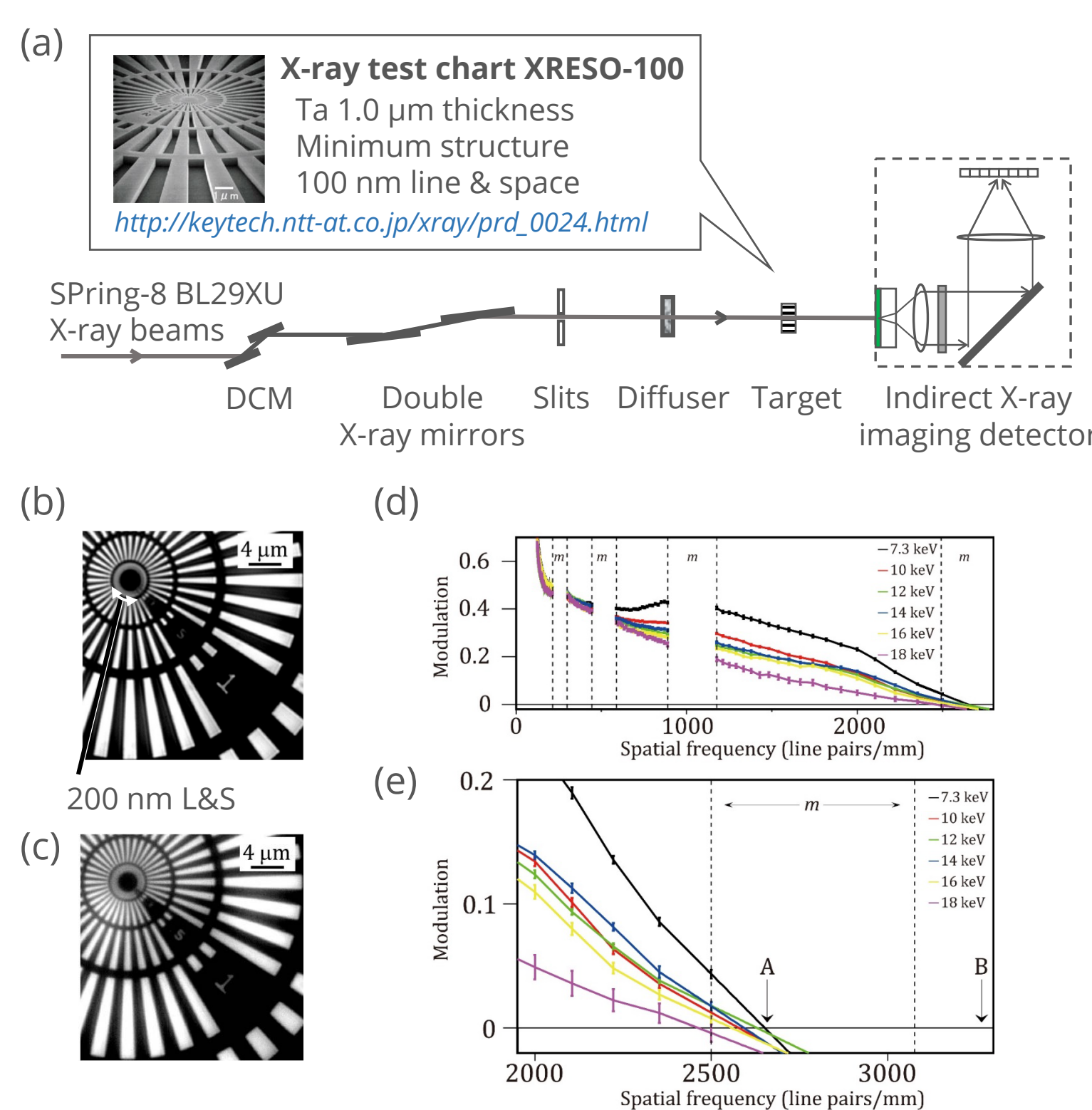


Fig. 4 (a) Schematics of experimental setup
(b) X-ray transmission image of test chart at 7.3 keV
(c) X-ray transmission image of test chart at 16 keV
(d) MTFs calculated from test chart images
(e) MTFs around the cutoff region

200 nm L&S structure was successfully visualized in the configuration of a 5 μm -thick LuAG:Ce scintillator and NA0.85 objective lens [1].

VLSI circuit visualization

- Sample information
 - Image sensor SOPHIAS
 - 200 nm process VLSI
 - 300 nm width & 600 nm-thick Al lines
 - 500 μm -thick Si chip

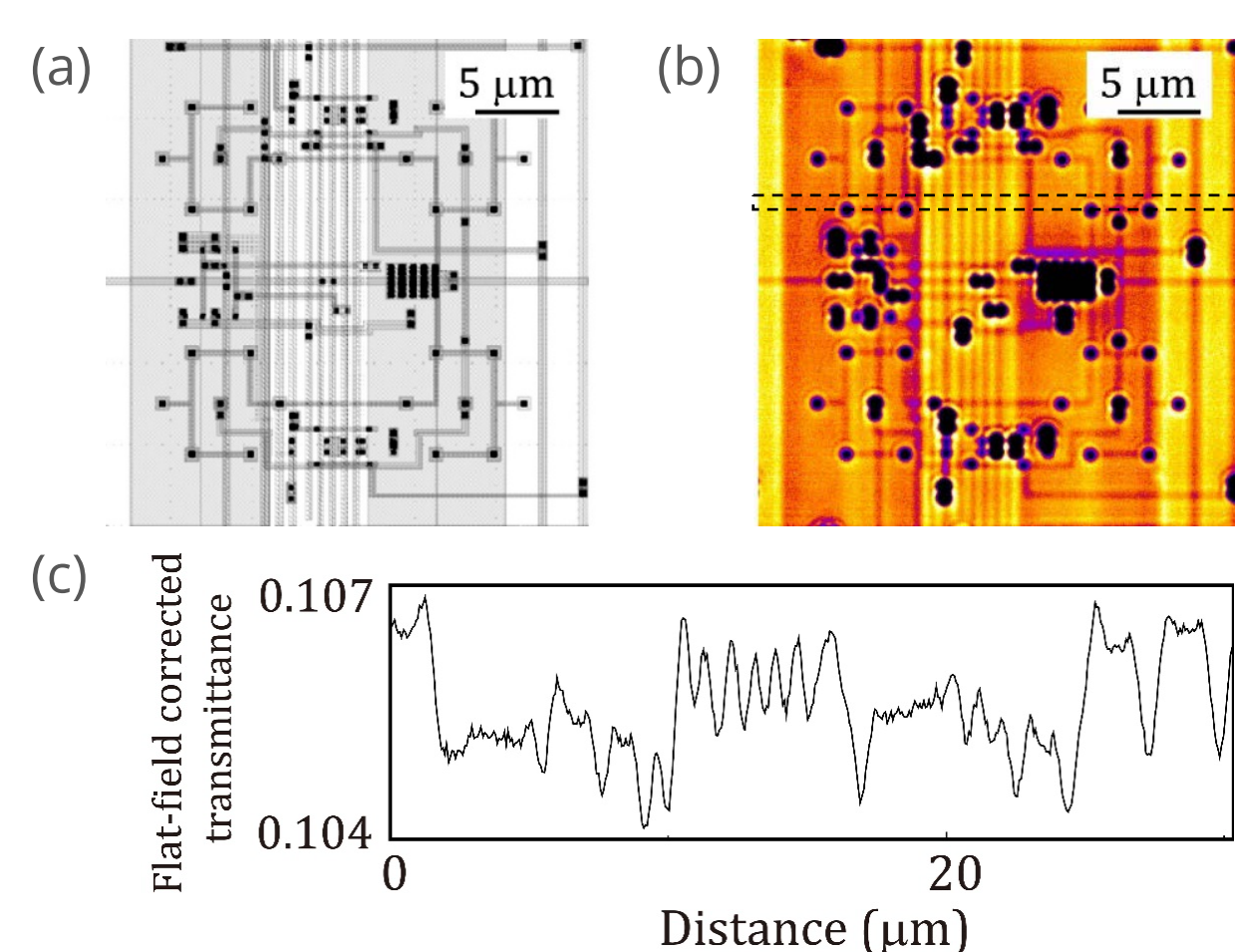


Fig. 5 (a) Circuit drawing of 200 nm process VLSI
(b) X-ray transmission image of (a)
(c) Projection of dashed rectangle in (b)

The sample has a 1000-times-thick Si substrate compared with Al wiring lines. Also, Si and Al are close in mass. In this low contrast condition, Al wiring lines implemented in the inner layer of the chip were successfully detected and visualized [1].

Deployment

Camera head design

- Standard unit
- Off-axis unit
- 5 μm -thick LuAG:Ce scintillator layer (min.)
- Scintillator replaceable
- Objective lens replaceable
- Camera optionality (c-mount)
- Proximity imaging design (min. 0.3 mm w.d.)
- Off-axis camera mount

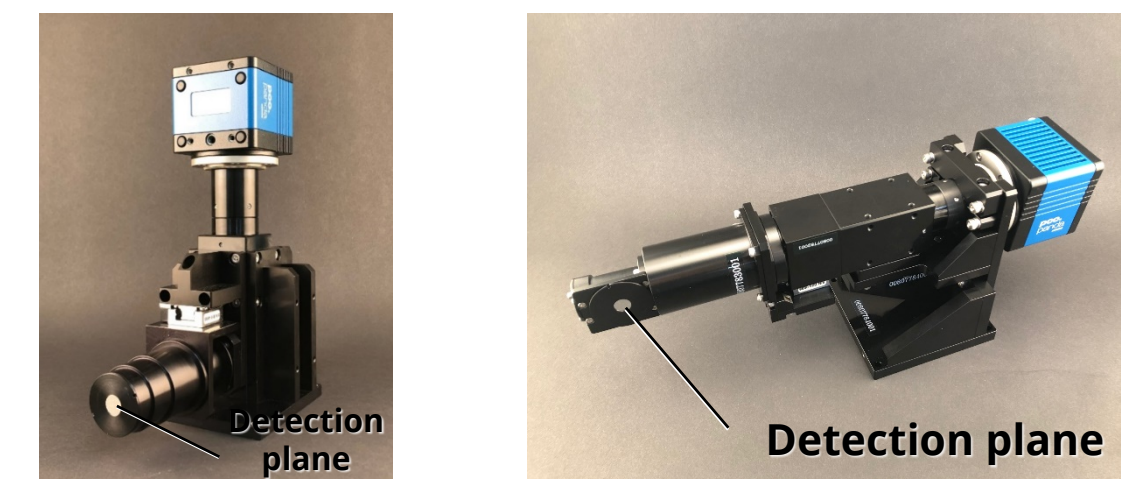


Fig. 6 Deployed imaging detectors

Optical configuration

Tab. 1 Optical configuration of deployed imaging detectors

		100x	50x	20x	10x	5x	2x
Resolution**	[μm]	~ 0.4	~ 0.5	~ 0.70	~ 1.1	~ 2.1	~ 5.3
Field of view**	[mm^2]	0.13 x 0.13	0.27 x 0.27	0.67 x 0.67	1.33 x 1.33	2.66 x 2.66	6.7 x 6.7
Conversion@10keV**	[e-/X-ray]	~ 12	~ 8	~ 3.2	~ 1.4	~ 0.35	~ 0.06

200 nm L&S visualization configuration

Objective line-up for Standard unit

Objective line-up for Off-axis unit

** Parameter is calculated using 2048 x 2048, 6.5 μm pixels

Two types of camera heads are deployed. The standard unit can be equipped with every objective and have a protruded detection plane to allow sufficient space for a sample holder. The off-axis unit can be mounted with the 2 ~ 20x objectives. The minimum depth size is designed to be short ~ 27 mm for detection plane insertion to narrow space.

Upgrade plan (enhancement of FOV)

Large format image sensor

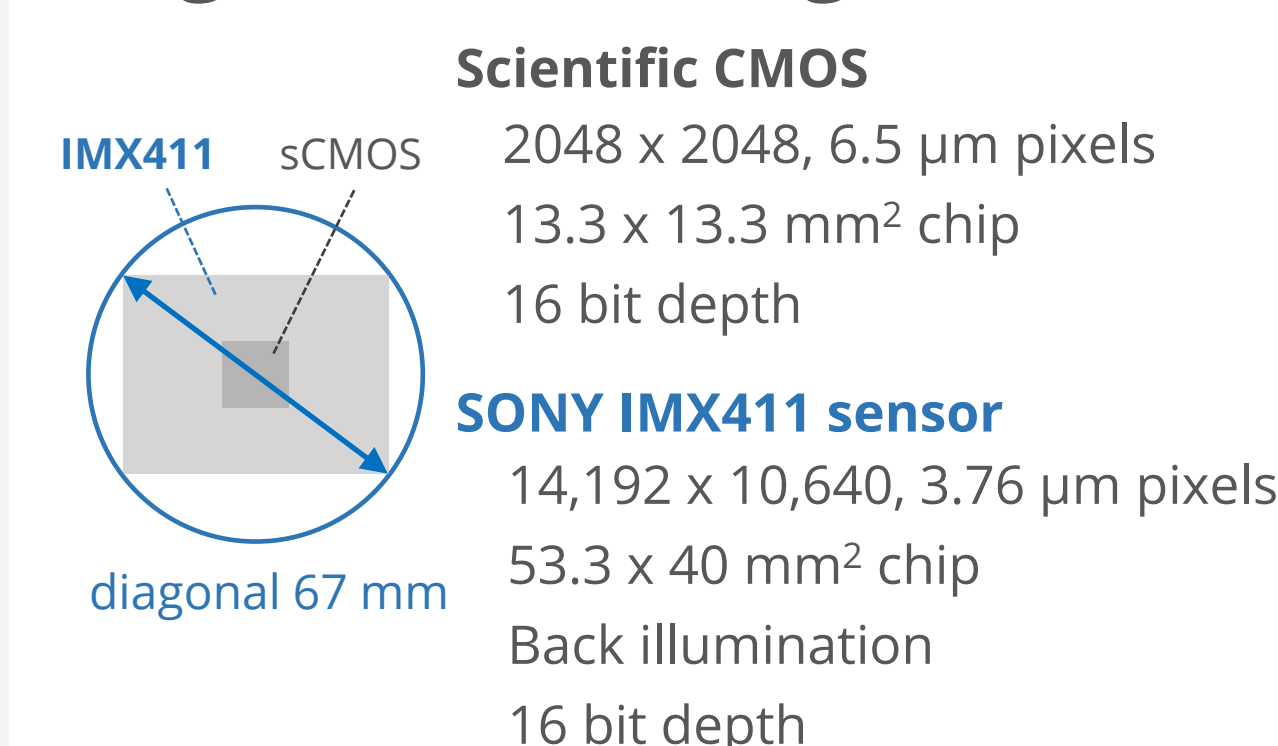


Fig. 6 Comparison between IMX411 & sCMOS

NA optimization

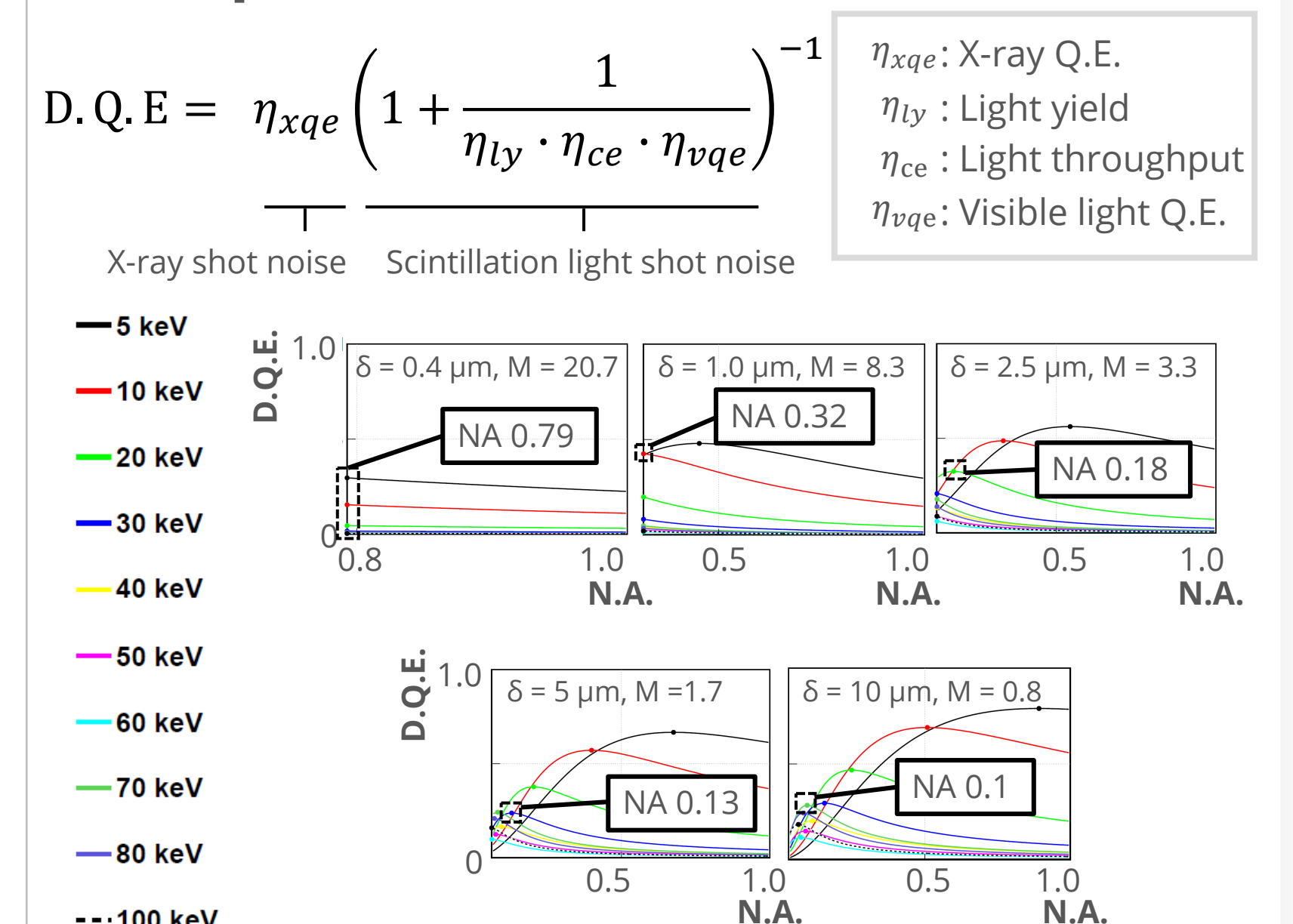


Fig. 8 DQEs as function of NA according to photon energies at 5 spatial resolution of 0.4 ~ 10 μm

Sampling optimization



Fig. 7 Schematic of sampling optimization

To increase spatial dynamic range, we are planning to implement the SONY IMX411 image sensor. An image circle of the optics is enlarged to be comparable with the IMX411 sensor diagonal by newly selecting or developing lenses. Sampling rate are also optimized to be 2 ~ 3 for the airy disk radius. Resulting FOV is expected to be ~ 20 times enhanced while keeping the spatial resolution. DQEs are calculated as function of NA, fixing spatial resolution and X-ray photon energy. Based on the DQE calculation results, we decide lens NA.

Estimated performance

Tab. 2 Optical configuration of upgraded imaging detectors

		Lens A1	Lens A2	Lens A3	Lens A4	Lens A5
Resolution	[μm]	~0.4	0.9	1.2	2.0	3.8
Field of view	[mm^2]	2.6 x 1.9	7.6 x 5.7	10.3 x 7.7	15.2 x 11.4	53.3x 40.0
Conversion	[e-/X-ray]	10.6 @ 10 keV	1.98 @ 10 keV	1.21 @ 10 keV	0.78 @ 20 keV	0.33 @ 30 keV
QE	[%]	17 @ 10 keV	63 @ 10 keV	81 @ 10keV	72 @ 20 keV	84 @ 30 keV
DQE	[%]	15 @ 10 keV	42 @ 10 keV	44 @ 10 keV	31 @ 20 keV	21 @ 30 keV

Development

Commercial off-the-shelf

Five optical configurations are planned to be deployed. With respect to around 1 ~ 5 μm resolution, the preferred performance can be achieved by utilizing commercial off-the-shelf lenses (Lens A2 ~ A5). We are planning to develop a dedicated imaging optics only for Lens A1.

Upgrade plan (enhancement of spatial resolution)

Solid immersion lens (SIL)

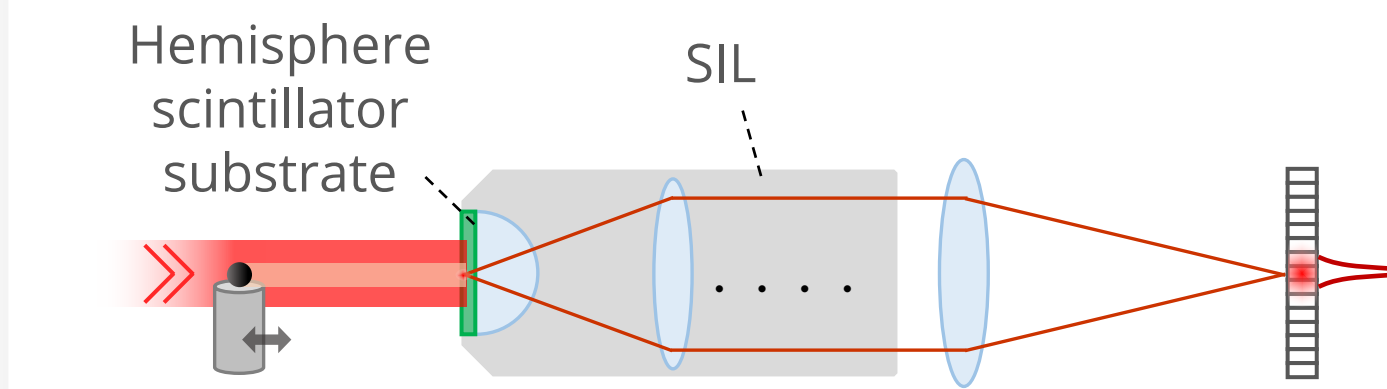


Fig. 9 Schematic of solid immersion lens configuration

The only way to enhance spatial resolution is to shorten the emission wavelength and/or to increase NA. We propose to develop a solid immersion lens with hemisphere scintillator. The NA is increased according to the refractive index of the scintillator (= ~ 1.85) and the resolution is improved to be ~ 200 nm resolution (100 nm L&S visualization).

Summary

Near-diffraction-limited resolution is achieved by the transparent thin-film LuAG:Ce scintillator development. The 200 nm line-and-space structure was successfully visualized. The indirect imaging detectors equipped with this scintillators are deployed to SACLA experiments and precise beam monitors. Various optical configuration are selectable for the resolution range of 0.4 ~ 3.25 μm . For the upgrade plans, the field of view is ~ 20 times enhanced by implementing the large format image sensor. The spatial resolution is improved to be 200 nm by constructing the solid immersion lens.

[1] T. Kameshima et al., *Optics Letters* 44, 1403 (2019)
 [2] A. Koch, C. Raven, P. Spanne, and A. Snigirev, *J. Opt. Soc. Am. A* 15, 1940 (1998).
 [3] S. M. Gruner, M. W. Tate, and E. F. Eikenberry, *Rev. Sci. Instrum.* 73, 2815 (2002).
 [4] K. Uesugi, Y. Suzuki, N. Yagi, A. Tsuchiyama, and T. Nakano, *SPIE Conf. Proc.* 4503, 291 (2002).
 [5] J. Touš, M. Horváth, L. Píňa, K. Blažek, and B. Sopko, *Nucl. Instrum. Methods Phys. Res., Sect. A* 591, 264 (2008).
 [6] J. Touš, K. Blažek, M. Nikl, and J. A. Mares, *J. Phys. Conf. Ser.* 425, 192017 (2013).
 [7] T. Martin and A. Koch, *J. Synchrotron Radiat.* 13, 180 (2006).
 [8] <https://www.sony-semicon.com/jp/e/products/IS/camera/product.html>